Food Chemistry: X 27 (2025) 102441

Contents lists available at ScienceDirect

Food Chemistry: X

journal homepage: www.sciencedirect.com/journal/food-chemistry-x

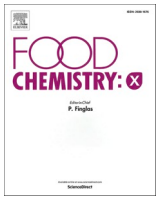

Fabrication and characterization of antioxidant fish oil Pickering emulsions stabilized by selenium nanoparticles-loaded whey protein concentrate and phloretin complex

Najme Kheynoor [a], Mohammad-Taghi Golmakani [a,*], Amir Mohammad Mortazavian [b,**], Elham Khanniri [c], Seyed Mohammad Hashem Hosseini [a]

[a] Department of Food Science and Technology, School of Agriculture, Shiraz University, Shiraz, Iran
[b] Department of Food Science and Technology, National Nutrition and Food Technology Research Institute, Faculty of Nutrition Sciences and Food Technology, Shahid Beheshti University of Medical Sciences, Tehran, Iran
[c] Department of Food Technology Research, National Nutrition and Food Technology Research Institute, Faculty of Nutrition Sciences and Food Technology, Shahid Beheshti University of Medical Sciences, Tehran, Iran

ARTICLE INFO

Keywords:
Antioxidant solid particles
Kilka fish oil
Milk
Oxidative stability
Selenium

ABSTRACT

This study aimed to enhance the nutritional value and oxidative stability of fortified milk by investigating the properties of fish oil Pickering emulsion (FOPE) stabilized by selenium nanoparticles (SeNP) loaded-whey protein concentrate/phloretin (WPC/PHL) complex. Initially, the influence of SeNP concentration on the WPC/PHL complex was evaluated through measurements of particle size, antioxidant activity, and intermolecular interactions. Results demonstrated that increasing SeNP concentration from 0.1 % to 0.3 % significantly enhanced the antioxidant activity, with ABTS assay values rising from 42.87 % to 76.14 % and DPPH assay values increasing from 59.10 % to 86.11 %. FTIR and docking analyses confirmed the formation of bonds (hydrogen and van der Waals) between the WPC/PHL/SeNP nanoparticles. Subsequently, the FOPEs were characterized, revealing that increasing SeNP concentration reduced droplet size, indicating improved emulsion stability. Furthermore, the oxidative stability of the emulsions improved with increasing SeNP concentrations (0.1 % to 0.3 %), as evidenced by a decrease in peroxide value (PV) from 4.27 meq/kgO_2 to 2.83 meq/kgO_2 and a reduction in malondialdehyde (MDA) content from 86.61 mg/kg oil to 62.78 mg/kg oil after 10 days of storage. Finally, the oxidative stability of fortified milk containing these FOPEs was also significantly enhanced. These findings provide a novel perspective on developing SeNP as an antioxidant particle, potentially suitable for formulating functional emulsified food products susceptible to oxidative deterioration.

1. Introduction

Functional foods are increasingly recognized for their potential to enhance human health through dietary interventions. Incorporating bioactive compounds like minerals, vitamins, and polyphenols into food systems is a promising strategy to improve nutritional and health benefits (Ju et al., 2020). Functional ingredients, particularly lipophilic compounds, benefit human health; however, their use in the food industry is limited due to their susceptibility to light, oxygen, and temperature during production, packaging, and storage (McClements, 2010).

Fish oil has a wide range of beneficial effects on human health such as preventing heart disease, anti-inflammatory effects, strengthening the immune system, improving nerves, and helping to improve depression and brain cognition. Therefore, fish oil has a high potential in the food and pharmaceutical industries (Chen et al., 2024). Food fortification with fish oil is challenging because of low water solubility, low bioavailability, and rapid oxidization of fish oil due to its high content of omega-3 long-chain polyunsaturated fatty acids (n-3 LC-PUFAs) such as eicosapentaenoic acid (EPA) and docosahexaenoic acid (DHA). These

* Corresponding author at: Department of Food Science and Technology, School of Agriculture, Shiraz University, Shiraz 7144165186, Iran.
** Corresponding author at: Department of Food Science and Technology, National Nutrition and Food Technology Research Institute, Faculty of Nutrition Sciences and Food Technology, Shahid Beheshti University of Medical Sciences, Tehran 193954741, Iran.
E-mail addresses: najme.kheynoor@shirazu.ac.ir (N. Kheynoor), golmakani@shirazu.ac.ir (M.-T. Golmakani), mortazvn@sbmu.ac.ir (A.M. Mortazavian), e.khanniri@sbmu.ac.ir (E. Khanniri), hhosseini@shirazu.ac.ir (S.M.H. Hosseini).

https://doi.org/10.1016/j.fochx.2025.102441
Received 19 February 2025; Received in revised form 3 April 2025; Accepted 4 April 2025
Available online 5 April 2025

challenges can be solved by antioxidants and advanced encapsulation technologies, which use colloidal delivery systems (Sepeidnameh et al., 2018).

One innovative approach to protect and deliver functional ingredients is Pickering emulsion (PE). PE, stabilized by food-grade solid particles at the oil and water interface, offers enhanced stability compared to traditional emulsions stabilized solely by chemical surfactants because solid particles can create physical and chemical barriers based on their characteristics (Keramat et al., 2022). Protein/polyphenol-stabilized PEs have gained great attention in recent studies. Incorporating polyphenols into protein molecules may create new bioactive complexes with multi-functional properties that can act as antioxidant emulsifiers (Gong et al., 2022). Adding polyphenols to proteins, either by partially replacing the protein or co-adsorbing them at the interface, improves the oxidative stability of emulsions. Incorporating antioxidants into solid particles is a novel strategy to accumulate them at the interface and improve the oxidative stability of PEs, though studies in this field are limited. Clove essential oil and α-tocopherol, when incorporated into solid particles, have been shown to reduce lipid oxidation in PEs (Keramat et al., 2022).

Whey protein concentrate (WPC) is a protein with both nutritional value and surfactant properties, making it suitable for use in delivery systems for bioactive compounds (Ks et al., 2017), and phloretin (PHL) as a polyphenol, a natural dihydrochalcone, can be used for its antidiabetic, antioxidant, anti-inflammatory, and antitumor activities (Mariadoss et al., 2019) were used in the current study. PHL combined with proteins can make more physical and oxidative stability for emulsions (Kheynoor et al., 2025).

Selenium is an essential trace element that supports health by participating in vital bodily processes. Selenium nanoparticles (SeNP) have low toxicity and act as an antimicrobial, anticancer, anti-inflammatory, and antioxidant agent. Conversely, selenium deficiency can lead to various diseases, including cardiovascular disorders, cancer, and infertility (Abdelhamid et al., 2024; Adadi et al., 2019; Mariadoss et al., 2022). Selenium plays a vital role in the immune system against viruses, such as COVID-19, and is essential for human health at certain stages of life such as pregnancy (Bae & Kim, 2020). Insufficient selenium in the human diet is related to plants grown (as the primary source of selenium) in selenium-poor soils (Adadi et al., 2019). Therefore, the design of selenium-enriched foods and supplements has become necessary. Recent studies have shown that SeNP, which is low in toxicity, can be used to fortify yogurt as an antibacterial agent (Alsuhaibani, 2018; Salama et al., 2021). It can be used for functional foods and beverages like milk (Adadi et al., 2019). Selenium content for 1 cup of milk with 1 % fat is six μg per serving, and selenium tolerable upper intake levels are up to 400 μg/day depending on age (https://ods.od.nih.gov/factsheets/Selenium-HealthProfessional/#en18). There have been few studies about the antioxidant properties of SeNP at different complexes (Alex et al., 2024; Nassar et al., 2023; Zhu et al., 2022), but the oxidative stability of the PEs by incorporating SeNP into protein/polyphenol complexes as solid particles has not been investigated yet. By incorporating SeNP into the WPC/PHL complex, we aim to create a multifunctional stabilizer that not only encapsulates fish oil but also provides additional antioxidant and nutritional benefits.

The novelty of this study is simultaneously encapsulating fish oil and SeNP as functional ingredients in the form of PE. The effect of different concentrations of SeNP, as an antioxidant, on WPC/PHL nanoparticles, FOPE, and fortified milk was investigated. The results of this work could be a guide for the use of SeNP as an essential trace element antioxidant in FOPE, thereby providing a theoretical basis for developing functional solid particles in emulsified foods containing n-3 LC-PUFAs content.

2. Materials and methods

2.1. Materials

Kilka fish oil without any added antioxidants was purchased from Apsa Pellet Company (Amol, Iran). Total tocopherol and α-tocopherol (vitamin E) content were 41.43 mg/kg, and 36.98 mg/kg, respectively. The peroxide value (PV) of the Kilka fish oil was <0.05 meq/kg. The fatty acid and tocopherol composition is shown in Table 1S. WPC 80 % (Hilmar, US), PHL (98 %) (Herba Diet Co., Rohtak, India), SeNP (Nanosadra Co., Mashhad, Iran), and all other reagents used were of analytical grade. Deionized water was used throughout the study.

2.2. Fabrication of WPC/PHL/SeNP complexes

WPC powder (5 % *w/v*) was weighed and dissolved in 100 mL of 10 mmol/L phosphate buffer (pH 7.0–7.2), followed by stirring magnetically at 4 °C overnight to promote complete hydration (Gong et al., 2022). Then, the WPC solution was mixed with SeNP (0.1 %, 0.2 %, and 0.3 % (*v*/v)) and stirred for 15 min. Then 0.014 g of PHL was added, magnetically stirred at 50 °C for 3 h, and stored at 4 °C overnight.

2.3. Fabrication of FOPE

FOPE was fabricated by homogenizing 20 % (*w*/w) fish oil with 80 % (w/w) WPC/PHL/SeNP complex solution prepared in the previous step. WPC/PHL nanoparticles containing 0.1 %, 0.2 %, and 0.3 % of SeNP were used to prepare FOPE1, FOPE2, and FOPE3 respectively. Also, FOPE made from the WPC/PHL nanoparticles (without SeNP) was considered control FOPE. Fish oil was added dropwise to the WPC/PHL/SeNP complex at 10,000 rpm for 2 min, followed by emulsification at 18,000 rpm for an additional 2 min.

2.4. Characterization of WPC/PHL/SeNP complexes and FOPE

2.4.1. TEM

TEM was used to observe the microstructure of WPC/PHL/SeNP complexes and their FOPE. All samples were stained with 100 μL of 0.5 % aqueous uranyl acetate solution and then air-dried completely. Images were obtained at 15 k magnification and 100 kV voltage (Zhu et al., 2022).

2.4.2. Determination of distribution size

The distribution size of WPC/PHL/SeNP complexes and FOPE at different concentrations of SeNP was characterized using a dynamic light scattering (DLS) particle size analyzer (Nanotrac Wave, Microtrac Inc., Montgomeryville, PA). The refractive index of oil was 1.467, and water was used as the dispersant (refractive index of 1.331). After production, measurements were made in triplicate.

2.4.3. In vitro antioxidant activity of WPC/PHL/SeNP complexes

2.4.3.1. ABTS radical scavenging activity. ABTS radical scavenging activity was measured based on the method described by Meng et al. (2022). Briefly, 7 mmol/L of ABTS aqueous solution was mixed with 2.45 mmol/L potassium persulfate aqueous solution at 1:2 volume ratio. Then, the mixture was incubated for 12 h at the dark room temperature. Adjusting the mixture with phosphate buffer solution (10 mmol/L, pH 7.0–7.2) to obtain absorbances of 0.7 ± 0.02 at 734 nm. Four mL of ABTS solution was blended with 0.1 mL of sample solution and vortexed vigorously. The absorbance of the sample solution was read at 734 nm. The ABTS radical scavenging activity was calculated according to the following equation:

$$\text{ABTS radical scavenging activity } (\%) = ((A_0 - A_1)/A_0) \times 100 \quad (1)$$

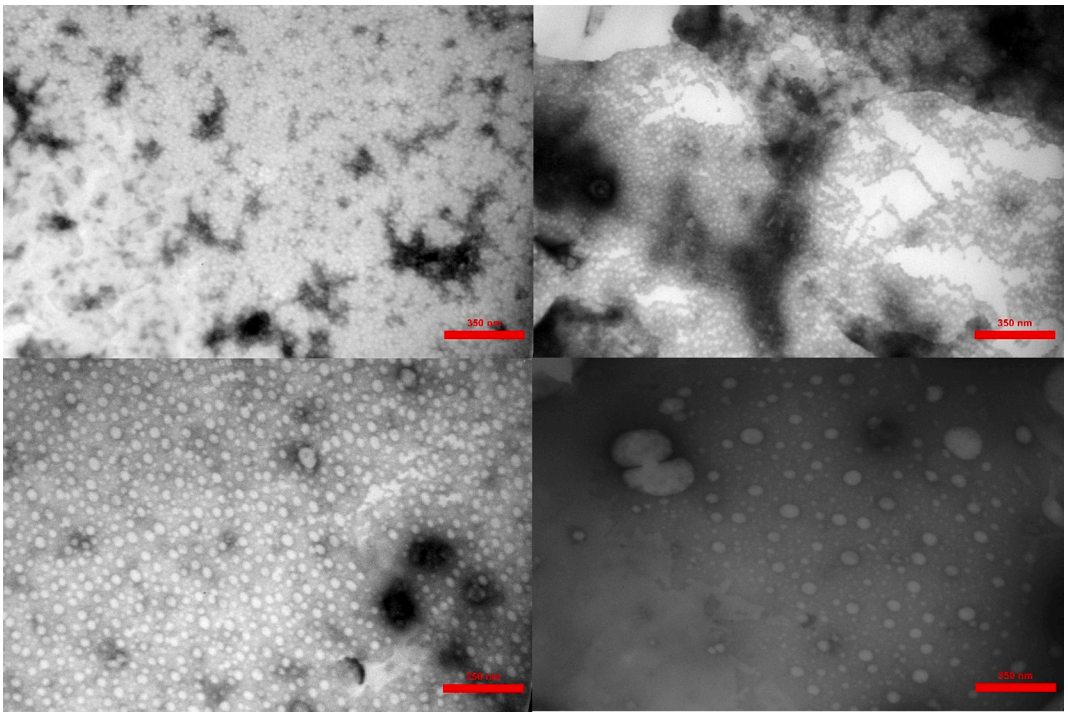

Fig. 1. Transmission electron microscopy (TEM) of whey protein concentrate/phloretin particles, (a) without selenium nanoparticles, (b) with 0.3 % (*v*/v) of selenium nanoparticles; TEM of fish oil Pickering emulsion made from (c) whey protein concentrate/phloretin particles, and (d) whey protein concentrate/phloretin particles containing 0.3 % (v/v) of selenium nanoparticles.

where A_1 and A_0 are the absorbance of the sample and the control, respectively.

2.4.3.2. DPPH radical scavenging activity measurement. The DPPH radical scavenging activities of WPC/PHL/SeNP complexes were measured according to the method previously reported by Gong et al. (2022) with some modifications. DPPH radical methanolic stock solution was prepared and diluted with methanol to obtain the 1.2 absorbance at 515 nm. Then, 1 mL DPPH radical stock solution was blended thoroughly with 0.2 mL of the sample and stored for 30 min at a dark room temperature. The absorbance of the sample solution was read at 515 nm. The DPPH radical scavenging activity was calculated according to the following equation:

$$\text{DPPH radical scavenging activity } (\%) = ((A_0 - A_1)/A_0) \times 100 \quad (2)$$

where A_1 and A_0 are the absorbance of the sample and the control, respectively.

2.4.4. The Fourier transform infrared (FTIR)

The chemical structure of the WPC/PHL/SeNP complexes was investigated using an FTIR spectrometer. Each solution was dried and ground into a homogeneous powder for recording FTIR spectra using a Nicolet Nexus 470 spectrometer (Thermo Fisher Scientific, Waltham, MA). The spectra were obtained at 500–4000 cm^{-1} wavenumbers at 4 cm^{-1} resolution.

2.4.5. Molecular docking

The molecular docking study facilitates the prediction of the binding interaction between the protein and small molecules (Baruah et al., 2022). The molecular docking simulation was done between PHL, SeNP, and β-lactoglobulin for the first time. The structures were downloaded for every material; β-lactoglobulin was selected as the model protein, the primary component of WPC protein. β-lactoglobulin (ID: 1B8E) from the Protein Data Bank archive (PDB) (http://www. rcsb.org/), SeNP (CID 6326970), and PHL (CID 4788) from PubChem database (https://pubchem.ncbi.nlm.nih.gov/) were downloaded. The protein structure was prepared for docking by adding hydrogens, assigning charges, and removing water molecules and other ligands present in the crystal structure using AutoDock Tools version 1.5.6. The ligand structure was also prepared by adding hydrogens and assigning charges using the same software. The docking simulations were carried out using the AutoDock Vina software version 1.2.0. The docking box was centered on the protein structure, covering the entire protein. The grid box size was X = 23.25 Y = 23.25 Z = 21.75, and the center was X = 11.874 Y = 20.747 Z = 38.65. The docking results were analyzed using AutoDock Tools. The hydrogen bonds, electrostatic, and van der Waals interactions were analyzed using Discovery Studio Visualizer version 20.1, Chimera X version 1.7, and LigPlot^{+} version 2.2.

2.4.6. Oxidative stability of FOPEs

Peroxide value (PV), as an indicator of the formation of primary lipid oxidation products, and the content of thiobarbituric acid reactive substances (TBARS), which indicates the formation of secondary lipid oxidation products, were measured at 4 °C after 1, 3, 7, and 10 days of production in FOPE. For the PV test, the oil was separated from FOPE by centrifugation at 3000 rpm for 30 min, and then the fat layer was collected from the surface using a spoon. PV content was determined by titration with sodium thiosulfate (Low, 1992). The TBARS *v*alue was calculated from a standard curve prepared by malondialdehyde (MDA) (Su et al., 2015).

2.5. Fortified of skim milk with FOPE

Sterilized raw skim milk was purchased from Pegah-e-Fars Dairy Company (Shiraz, Iran). Freshly prepared FOPE without SeNP (control) and FOPE with the highest SeNP content (0.3 %, *v*/v) were added to sterile milk in a 1:10 (*v*/v) ratio to reach the recommended level of 300 mg EPA + DHA/100 mL (Yang et al., 2024). Then, they were transferred into aseptic bottles, mixed at 21 °C using an orbital shaker at 500 rpm to obtain a homogeneous dispersion, and kept at 4 °C for ten days.

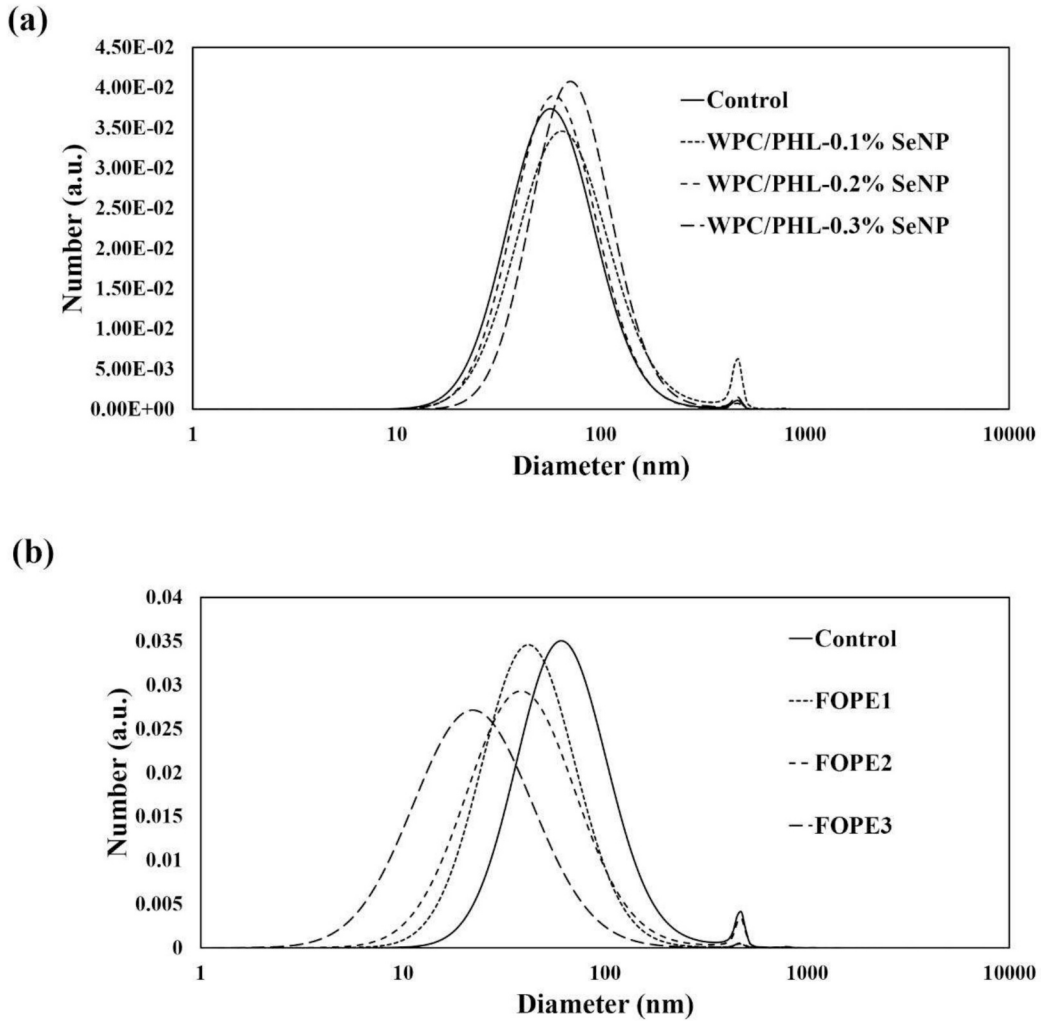

Fig. 2. Droplet size distribution of (a) whey protein concentrate/phloretin (WPC/PHL) at different concentrations of selenium nanoparticles (SeNP) and (b) fish oil Pickering emulsion (FOPE), (FOPE1, FOPE2, and FOPE3 made from WPC/PHL containing 0.1 %, 0.2 %, and 0.3 % (v/v) SeNP respectively).

2.5.1. Oxidative stability of fortified milk

The fortified milk with FOPE without SeNP was used as a control and compared to the fortified milk with FOPE with the highest SeNP content (0.3 %, v/v). The PV level was determined according to Yang et al. (2024), with some modifications. Briefly, 0.3 mL of extracted oil was added into 7.7 mL of chloroform: methanol (7:3, v/v) and vortexed for 10 s. Then, 50 μL of ammonium thiocyanate solution and 50 μL of ferrous chloride solution were added and vortexed for 10 s. After incubating (21 °C, 20 min) in the dark, the absorbance of the milk samples was measured at 505 nm with a UV/Vis spectrophotometer (Evolution 201, Thermo Fisher Scientific, Waltham, MA). The external calibration of cumene peroxide was used to determine the peroxide concentration in the milk samples. The MDA level was determined according to Cilliers et al. (2014). Precisely, 1.5 mL of 1 g/mL trichloroacetic acid (TCA) and 2 mL of 95 % ethanol were added to 20 mL milk samples. After incubating at 30 °C for 5 min, the samples were filtered with Whatman No.3 filter paper, the removed precipitates, then 1.45 % 2-thiobarbituric acid solution (1 mL) was added, and incubated at 80 °C for 60 min. After that, the samples were cooled to room temperature and centrifuged (4000 rpm, 15 min). Finally, the absorbance was read at 532 nm with a UV/Vis spectrophotometer, and the MDA level was expressed in mg/kg of milk. The external calibration of tetraethoxypropane (TEP) as a standard was used to determine the MDA concentration in the milk samples.

2.5.2. Color

The color of each sample was measured via a Chromameter (ColorFlex, Reston, AV). The CIELAB scale L^* (whiteness), a^* (redness-greenness), b^*(yellowness-blueness), H (hue angle), C (chroma), and ΔE (color changes) (Gulzar et al., 2020) were measured, to compare the fortified milk with FOPE without SeNP and the fortified milk with FOPE with the highest SeNP content.

2.6. Statistical analysis

All measurements were carried out in triplicate. The analysis was achieved using SPSS 24 software. The mean ± standard deviation of data is presented. Variance (ANOVA) analysis was performed, and Duncan's multiple range tests were used for mean comparison. Time-dependent data were analyzed using the repeated measurement test. The significant level was considered to be $P < 0.05$.

3. Results and discussion

3.1. Characteristics of WPC/PHL/SeNP complexes and FOPEs

3.1.1. TEM

The effect of SeNP on the morphology of WPC/PHL/SeNP complexes and their FOPE is highlighted in the TEM images presented in Fig. 1. The TEM images were taken 3 days after production. The WPC/PHL/SeNP

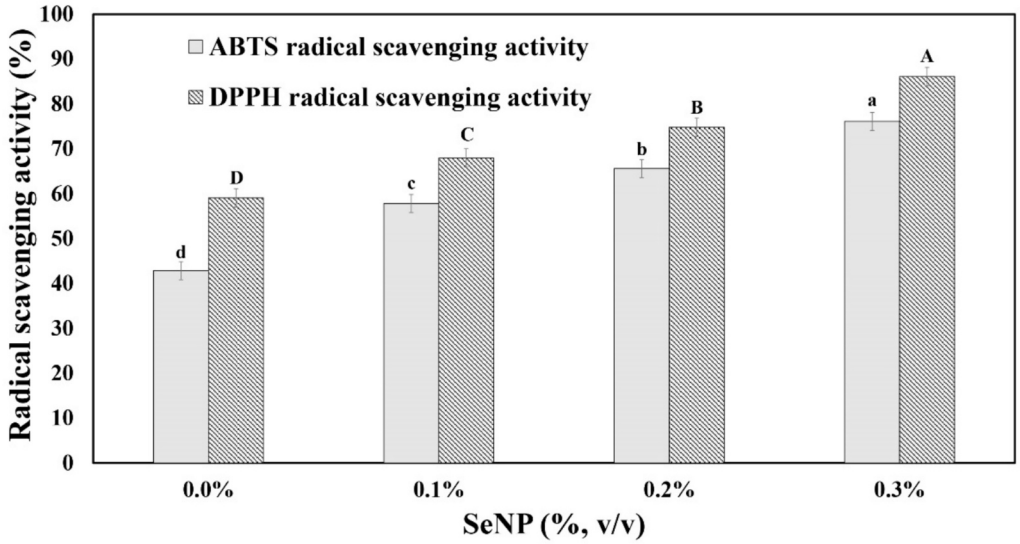

Fig. 3. ABTS and DPPH radical scavenging activity (%) of whey protein concentrate/phloretin at different concentrations of selenium nanoparticles (SeNP); different superscript letters indicate the difference between the samples ($P < 0.05$).

complexes without SeNP, well-separated spherical nanoparticle structures presenting particle sizes below 100 nm were observed (Fig. 1a). By the addition of 0.3 % (*v*/v) SeNP, clumpy aggregates were noticed between nanoparticles, which can increase their size (Fig. 1b). Similarly, Abdelhamid et al. (2024) reported that, at high SeNP concentrations, chitosan nanoparticles may exhibit larger particle sizes by forming aggregates. TEM images of FOPEs (Fig. 1c and Fig. 1d) showed droplets are spherical and relatively uniform, with an increase in droplet size of FOPE3 compared to the control. This increase in droplet size suggests droplet coalescence during time and limitation in long-storage FOPE stability containing SeNP.

3.1.2. *Distribution size of WPC/PHL/SeNP complexes and FOPEs*

Fig. 2 and Table. 2S show the size distribution and particle size of WPC/PHL/SeNP complexes and their FOPE samples at different concentrations of SeNP after production. With increasing SeNP, the particle size and size distribution of the WPC/PHL/SeNP complexes increased slightly, and the droplet size and size distribution of FOPEs decreased ($P < 0.05$). The particle size of WPC/PHL/SeNP complexes with 0.0 %, 0.1 %, 0.2 %, and 0.3 % (*v*/v) of SeNP was 66.75 nm, 58.40 nm, 68.26 nm, and 82.27 nm, respectively which shows an increasing trend. The increase in the size of WPC/PHL/SeNP complexes can be attributed to aggregation caused by SeNP, as observed in their TEM images (Section 3.1.1). On the other hand, the droplet size of FOPE with 0.0 %, 0.1 %, 0.2 %, and 0.3 % (v/v) of SeNP was 77.74 nm, 49.53 nm, 53.39 nm, and 29.32 nm, respectively which shows a decreasing trend. The size reduction of the FOPE droplets with increasing concentration of SeNP (after production) is associated with locating more particles at the interface, and more coverage droplets. However, according to TEM images (Section 3.1.1), after 3 days, the increasing aggregation of SeNP

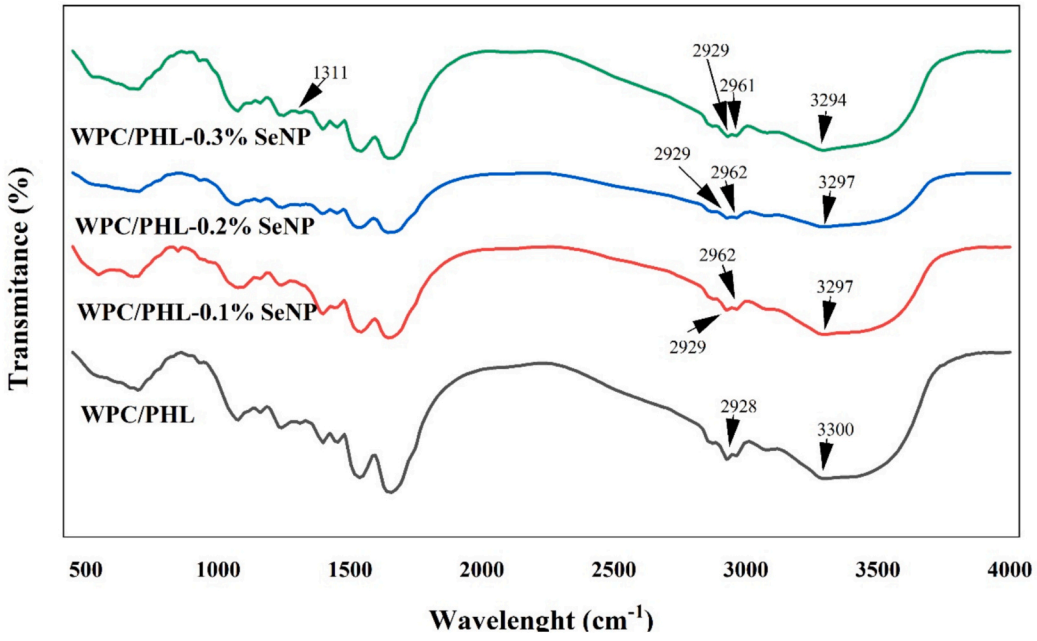

Fig. 4. Fourier transform infrared (FTIR) spectroscopy of whey protein concentrate/phloretin (WPC/PHL) at different concentrations of selenium nanoparticles (SeNP).

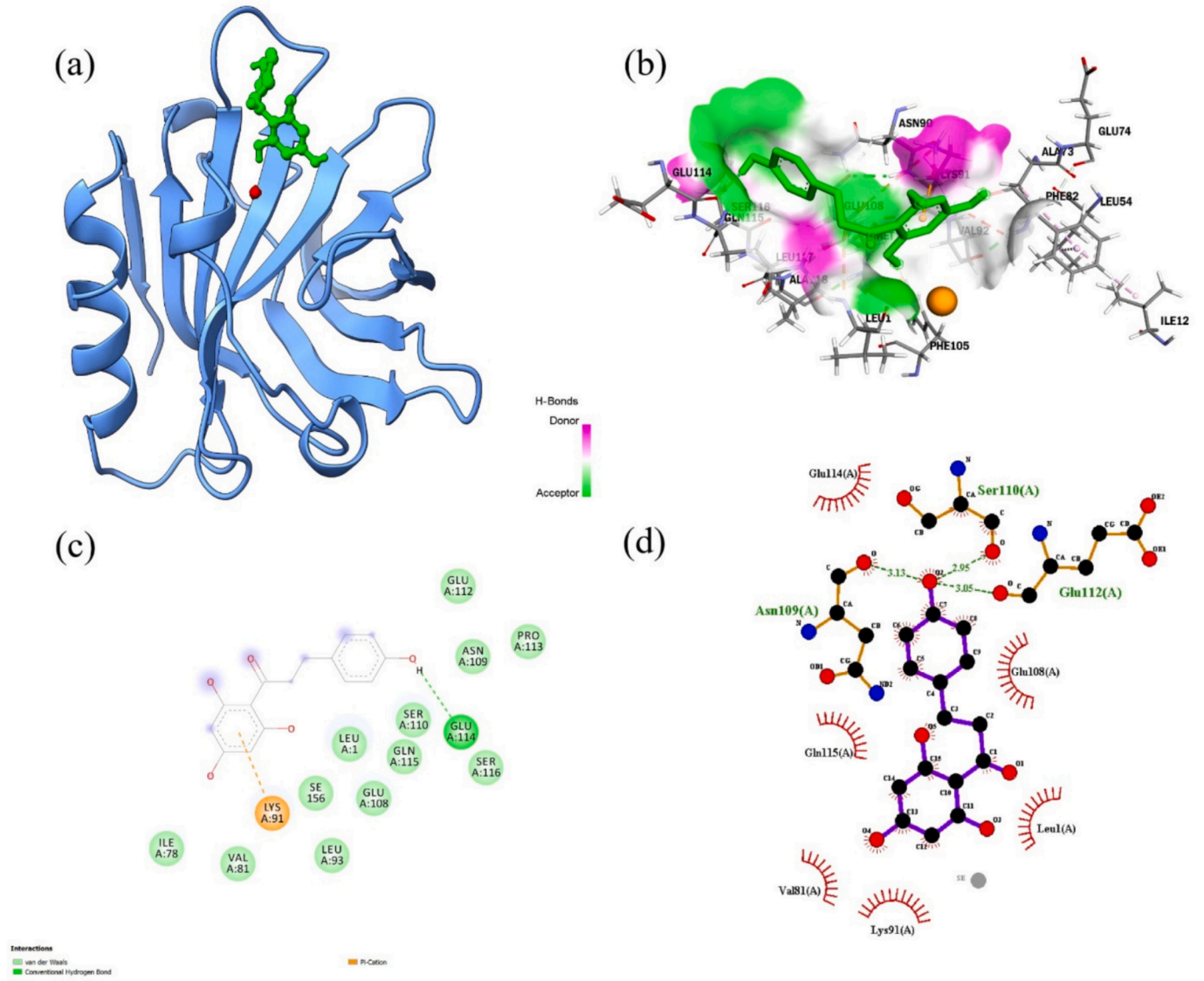

Fig. 5. Molecular docking between β-lactoglobulin, selenium nanoparticles, and phloretin. (a) 3D structure of the complex, (b) hydrogen bond surface between amino acid residues of protein active sites, selenium nanoparticles, and phloretin, where the purple and green color respectively represent H-bond donor and acceptor, (c) and (d) 2D schematic interaction diagram. (For interpretation of the references to color in this figure legend, the reader is referred to the web version of this article.)

located on the surface of droplets leads to particle coalescence. This coalescence causes an increase in the droplet size and a decrease in the stability of FOPE.

3.1.3. Antioxidant activity

It is widely recognized that SeNP regulates the levels of antioxidant substrates and the antioxidant enzyme activity, thereby serving as a vital defense against oxidative damage to both humans and animals (Bai et al., 2017). The radical scavenging activity of WPC/PHL/SeNP complexes was investigated by ABTS and DPPH methods (Fig. 3) calculated according to Eq. (1) and Eq. (2), respectively. The ABTS radical scavenging activity for WPC/PHL/SeNP complexes with 0.0 %, 0.1 %, 0.2 %, and 0.3 % (v/v) of SeNP was 42.87 %, 57.83 %, 65.62 %, and 76.14 %, and the DPPH radical scavenging activity was 59.10 %, 67.98 %, 74.83 %, and 86.11 %, respectively. Results showed that the antioxidant activity of the samples was dependent on SeNP concentration ($P < 0.05$), with higher SeNP concentrations exhibiting higher radical scavenging activity. Similarly, the radical scavenging activity of green SeNPs synthesized using the endophytic fungal strain *Penicillium verhagenii* (Nassar et al., 2023), and *Emblica officinalis* fruit extract (Gunti et al., 2019) increased proportionally with SeNP concentration. Also, He et al. (2023) reported that encapsulated selenium-enriched peptide by dextran/whey protein isolate could increase the DPPH and ABTS radical scavenging activities. A similar study showed that SeNP has antioxidant activity at low concentrations (Nassar et al., 2023). The antioxidant activity of SeNP could be attributed to the inhibition and neutralization of free radicals formation via electron transfer. Also, it could be attributed to the unique properties of its nanoparticles scale, which are exceptionally high surface area to size that may increase their antioxidative action (Nassar et al., 2023). In addition, SeNPs can act as antioxidant activity at the interface (adsorbed particle) or in the continuous phase (unadsorbed particle). Therefore, SeNP, as an antioxidant with health properties, can be used along with solid particles to improve the chemical stabilization of FOPE for functional foods.

3.1.4. FTIR

FTIR can be used to identify structural changes in functional groups located on the surface of nanoparticles through the analysis of

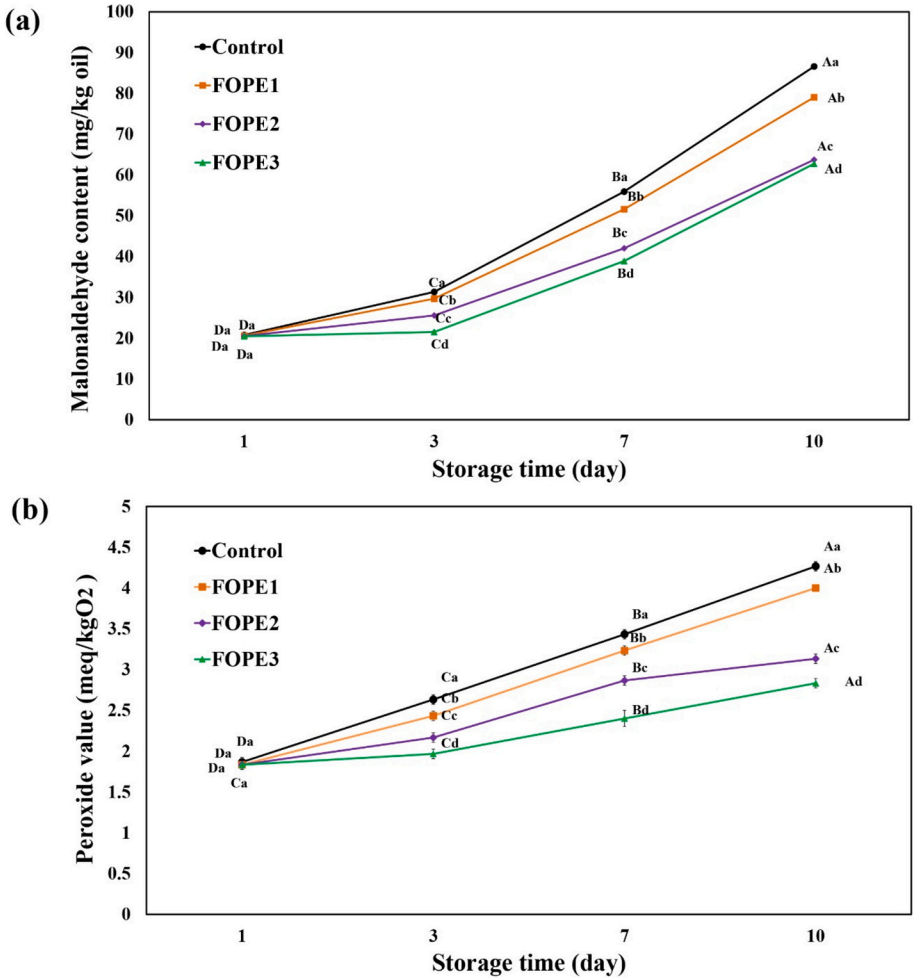

Fig. 6. (a) Malondialdehyde and (b) peroxide value of fish oil Pickering emulsions (FOPE), (FOPE1, FOPE2, and FOPE3 made from whey protein concentrate/phloretin containing 0.1 %, 0.2 %, and 0.3 % (v/v) selenium nanoparticles respectively during storage; different uppercase letters indicate the difference during storage and different lowercase letters indicate the difference between the sample types ($P < 0.05$).

vibrational frequencies of chemical bonds (Gunti et al., 2019). In particular, FTIR makes it possible to investigate the structural changes of proteins caused by changes in the surrounding environment. Such information is taken out by correlating the frequencies of amide states to specific types of hydrogen bonding patterns that characterize the secondary structural elements of polypeptide chains such as α-helix, β-sheet, beta-turn, and random coil (Stani et al., 2020). Fig. 4 represents the FTIR results of WPC/PHL/SeNP complexes at different concentrations of SeNP. The FTIR spectrum of control showed strong absorption bands at 3300, 2928, 1651, 1536, 1450, 1396, 1239, 1159, 1074, and 699 cm^{-1}. Similarly, the FTIR spectrum of WPC/PHL-0.3 % SeNP showed strong absorption bands at 3294, 2961, 2929, 1653, 1538, 1450, 1396, 1311, 1240, 1159, 1074, and 698 cm^{-1}. The peak at 3300 cm^{-1} for control is assigned to the N—H stretching vibration of the amide I from WPC; this peak was slightly shifted to the left (redshift) to 3297, 3297, and 3294 cm^{-1} for WPC/PHL nanoparticles with 0.1 %, 0.2 %, and 0.3 % (*v*/v) of SeNP, respectively. This redshift could be related to the increase of the hydrogen bond and a decreased number of the free hydroxyl group (He et al., 2023). The peaks at 1651 and 1536 cm^{-1} are attributed to the C═O of amide I and C-N-H of amide II, respectively, that sufficiently characterize the whey proteins. In the samples containing SeNP, which is a peak of 2961–2 cm^{-1} (corresponding to -CH_2 groups), which is absent in the sample without SeNP, suggesting the presence of hydrophobic interactions of SeNP via polyphenol rings of PHL and hydrophobic pockets of WPC (Jia et al., 2019). These hydrophobic interactions help create a network that can increase the stability of the structure and help improve antioxidant activity. Also, SeNP can act as a catalyst that enhances antioxidant activity. In addition, WPC/PHL-0.3 % SeNP peaked at 1311 (attributed to amide III), which was not observed in other samples, indicating the formation of a new bond. The amide III band is mainly associated with CN stretching, NH bending vibrations, CC stretching, and CH bending. The wavelength at 1311 cm^{-1} could demonstrate the Amide III band, which can be attributed to the characteristic Cx = Ox….H-N inter-strand hydrogen bond in the triple-helix (Stani et al., 2020). Therefore, SeNPs by hydrophobic interactions and hydrogen bond interactions with WPC and PHL. Hydrophobic interactions and hydrogen bonds can lead to the creation of a stable structure that can keep antioxidant activity or even improve it.

3.1.5. *Molecular docking*

The molecular docking could indicate the interaction between polyphenol and protein molecules. Molecular docking calculations were used to systematically and computationally search for the most likely binding conformations of β-lactoglobulin, SeNP, and PHL. In this regard, β-lactoglobulin was considered a representative WPC compound. The results of the molecular docking simulation with the lowest binding energy are displayed in Fig. 5a. According to the schematic diagram of PHL, SeNP, and β-lactoglobulin (Fig. 5d), hydrogen bonding interaction played an essential role in the formation of PHL, SeNP, and β-lactoglobulin complexes as confirmed by the results of FTIR (section 3.1.4). Hydrogen bonds in WPC/PHL/SeNP complexes can help strengthen interactions and increase the stability and antioxidant activity of the

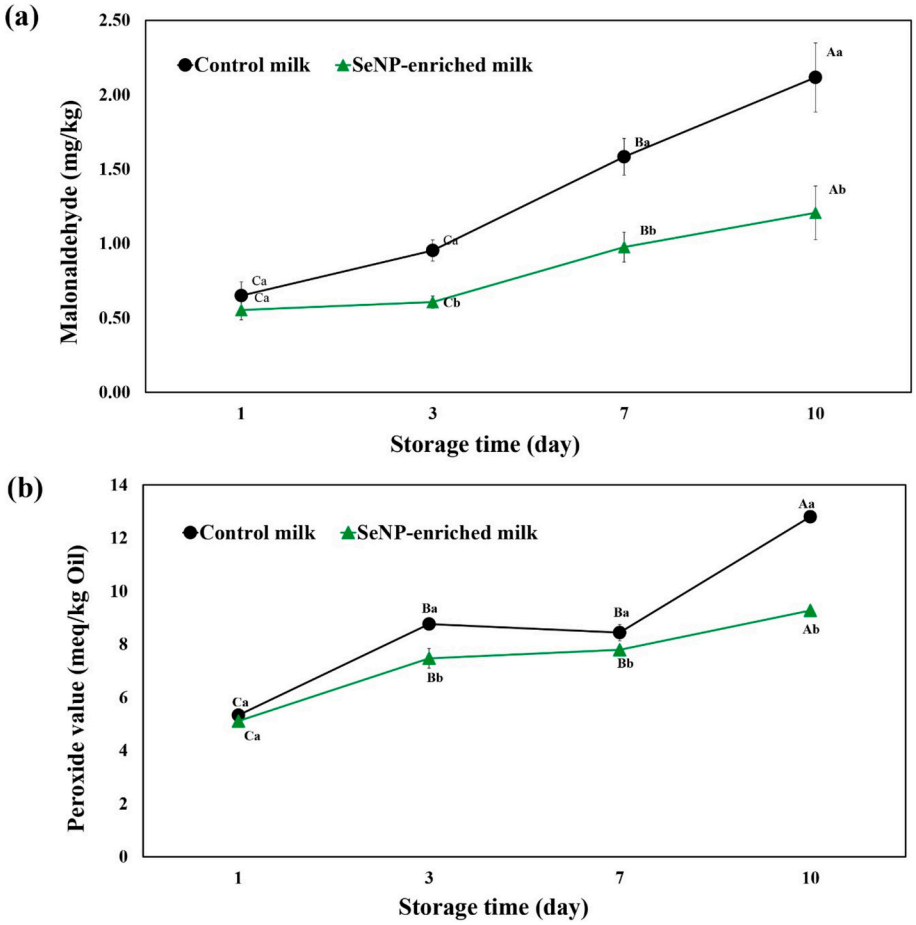

Fig. 7. (a) Malondialdehyde content and (b) peroxide value of control and SeNP-enriched milk during storage; different uppercase letters indicate the difference during storage, and different lowercase letters indicate the difference between the sample types ($P < 0.05$).

complexes. The detailed binding regions and groups between PHL, SeNP, and β-lactoglobulin are shown in Fig. 5 b-d. The hydrogen bonds, Pi-cation, and van der Waals forces were found between β-lactoglobulin, SeNP, and PHL. Amino acid residues involved in hydrogen bonds are Glu 112, Ser 110, and Asn 109 represented in Fig. 5d, and Glu 114 in Fig. 5c. The Pi-Cation and Pi-donor hydrogen bonds were found between the amino acid residues of β-lactoglobulin (Lys 91) and PHL (Fig. 5c). Similar forming hydrogen bonds have been reported in the interaction of polyphenols with pea protein (Zhang et al., 2022) and quinoa protein (Liu et al., 2021). Polyphenols contain phenolic hydroxyl groups capable of creating hydrogen bonds with protein carboxyl groups since they act as hydrogen donors (Zhang et al., 2022). In addition, Van der Waals bonds were detected for PHL with β-lactoglobulin and SeNP represented in Fig. 5c. Van der Waals bonds also play a role in the interactions between WPC, PHL, and SeNP. Although, these bonds are weaker than hydrogen bonds, can help stabilize the final structure and enhance the stability of the PEs. This can lead to reduced oxidation and increased shelf life of the emulsified products. Hydrogen and *v*an der Waals bonds can help improve the permeability and accessibility of SeNP to the interface which can increase antioxidant efficacy.

3.1.6. *Oxidative stability of FOPEs*

The Kilka fish oil used in this study contains 20.32 % omega-3, with the largest portion being DHA at 11.87 % (Table 1S). Therefore, it is necessary to monitor fish oil oxidation stability in emulsion and fortified milk to maintain its nutritional value. The oxidative stability of the FOPEs was assessed by measuring the MDA content (Fig. 6a) and PV value (Fig. 6b). The MDA content of FOPEs at different SeNP concentrations ranged from 20 to 21 mg/kg oil, while the PV content ranged from 1.8 to 1.9 meq/kg O_2 after one day of storage. After ten days of storage, the MDA content of control, FOPE1, FOPE2, and FOPE3 reached 86.61 (mg/kg oil), 79.06 (mg/kg oil), 63.75 (mg/kg oil), and 62.78 (mg/kg oil), respectively. As well, the PV content of control, FOPE1, FOPE2, and FOPE3 reached 4.27 meq/kgO_2, 4.00 meq/kgO_2, 3.13 meq/kgO_2, and 2.83 meq/kgO_2 after ten days of storage. Results show the content of MDA and PV of FOPEs have increased over time and decreased by increasing the amount of SeNP ($P < 0.05$). Therefore, the use of SeNP had a positive effect on the oxidative stability of FOPEs. The WPC/PHL/SeNP nanoparticles formed an antioxidant film at the interface of FOPEs to inhibit the oxidation processes. This increase in oxidative stability with increasing SeNP concentration can be due to more SeNP as an antioxidant at the interface area, consistent with the results of antioxidant activity (section 3.1.3). Similarly, the microencapsulation of selenium by the Arabic/Persian gum complex increased the oxidative stability of soybean oil (Jalalizand & Goli, 2021).

The high initial amount of oxidation indices (MDA and PV) of FOPEs with and without SeNP can be related to the high sensitivity of fish oil and the emulsion production method. Kilka fish oil is susceptible to oxidation due to its polyunsaturated fatty acids, represented in Table 1S. The use of Ultraturrax by generating high heat and kinetic movement could be the second reason for the high initial content of PV and MDA in FOPEs (Ghelichi et al., 2023).

3.2. *Characteristics of fortified milk*

3.2.1. *Oxidative stability of fortified milk*

The oxidative stability of milk fortified with FOPE without SeNP (control) and FOPE made from WPC/PHL-0.3 % (*v*/v) of SeNP was

assessed by the content of MDA (Fig. 7a) and PV (Fig. 7b) at 4 °C for ten days. SeNP-enriched milk had significantly higher oxidative stability than the control milk after ten days of storage ($P < 0.05$). The MDA value of SeNP-enriched milk (1.21 mg/kg) was significantly lower than control milk (2.12 mg/kg) after ten days of storage (Fig. 7a). Similar oxidation behavior was observed in the case of PV, as indicated in Fig. 7b. The PV content of SeNP-enriched milk remained below <9.27 meq/kg oil after ten days of storage but in control milk, PV content reached 12.8 meq/kg oil. Previously, Wang et al. (2011) reported a lower PV in milk enriched with fish oil loaded into solid lipid particles compared to free fish oil. It is advised that the PV content in an edible food product should not surpass 30 meq/kg oil (Wang et al., 2011). Fish oil in both milk samples, with or without SeNP, remained stable after ten days, demonstrating the high efficiency of fish oil encapsulated by PEs. Also, incorporating SeNP into FOPEs as antioxidants enhanced the oxidative stability of the fortified milk.

3.2.2. Color attribute

The color attributes of fortified milk are presented in Table 2S. The b^* (as an indicator of yellowness-blueness) and C (chroma intensity) values of SeNP-enriched milk increased significantly ($P < 0.05$); however, a^*, H, L^*, and ΔE values were not significantly affected. SeNP-enriched milk showed lower whiteness compared to control milk. However, the application of SeNP had no adverse effect on the color acceptability of the fortified milk.

4. Conclusion

This study used SeNPs-loaded WPC/PHL complexes and created novel antioxidant solid particles used as stabilizers for FOPEs. PEs containing fish oil and SeNP as bioactive compounds used to fortify milk as a functional food. The antioxidant activity of WPC/PHL/SeNP complexes increased by increasing SeNP concentration. FTIR and docking results confirmed the forming of hydrogen bonds and van der Waals interaction between the WPC/PHL/SeNP nanoparticles. The results of TEM images and particle size distributions demonstrated that SeNP made particle aggregation during storage, and decreased the emulsion stability by increasing droplet size. With increasing SeNP concentrations, the MDA and P*V* content of FOPEs decreased and oxidative stability of FOPEs improved. Oxidative stability of fortified milk with FOPEs containing SeNPs results showed a lower oxidation rate ($P < 0.05$). Therefore, loading SeNP into solid particles enhanced the oxidative stability of FOPEs and improved the nutritional value of fortified milk due to the presence of SeNP and n-3 LC-PUFAs. These findings may provide a new approach to developing SeNP as an antioxidant particle and a nutritional ingredient for the formulation of functional emulsified food products.

CRediT authorship contribution statement

Najme Kheynoor: Writing – original draft, Visualization, Software, Methodology, Investigation, Formal analysis, Data curation, Conceptualization. **Mohammad-Taghi Golmakani:** Writing – review & editing, Visualization, Validation, Supervision, Software, Resources, Project administration, Funding acquisition, Conceptualization. **Amir Mohammad Mortazavian:** Validation, Supervision, Resources, Project administration. **Elham Khanniri:** Writing – review & editing. **Seyed Mohammad Hashem Hosseini:** Supervision.

Declaration of competing interest

The authors declare that they have no known competing financial interests or personal relationships that could have appeared to influence the work reported in this paper.

Acknowledgments

This research project was financially supported by Shiraz University.

Appendix A. Supplementary data

Supplementary data to this article can be found online at https://doi.org/10.1016/j.fochx.2025.102441.

Data availability

Data will be made available on request.

References

Abdelhamid, A. E., Ahmed, E. H., Awad, H. M., & Ayoub, M. M. (2024). Synthesis and cytotoxic activities of selenium nanoparticles incorporated nano-chitosan. *Polymer Bulletin, 81*(2), 1421–1437. https://doi.org/10.1007/s00289-023-04768-8

Adadi, P., Barakova, N. V., Muravyov, K. Y., & Krivoshapkina, E. F. (2019). Designing selenium functional foods and beverages: A review. *Food Research International, 120*, 708–725. https://doi.org/10.1016/j.foodres.2018.11.029

Alex, A., Biju, T. S., Francis, A. P., Veeraraghavan, V. P., Gayathri, R., & Sankaran, K. (2024). Quercetin-coated biogenic selenium nanoparticles: Synthesis, characterization, and in-vitro antioxidant study. *Advances in Natural Sciences: Nanoscience and Nanotechnology, 15*(1), Article 015012. https://doi.org/10.1088/2043-6262/ad2c7a

Alsuhaibani, A. M. (2018). Functional role of selenium-fortified yogurt against aflatoxin-contaminated nuts in rats. *Agriculture & Food Security, 7*, 1–12. https://doi.org/10.1186/s40066-018-0171-7

Bae, M., & Kim, H. (2020). The role of vitamin C, vitamin D, and selenium in immune system against COVID-19. *Molecules, 25*(22), 5346. https://doi.org/10.3390/molecules25225346

Bai, K., Hong, B., Hong, Z., Sun, J., & Wang, C. (2017). Selenium nanoparticles-loaded chitosan/citrate complex and its protection against oxidative stress in D-galactose-induced aging mice. *Journal of Nanobiotechnology, 15*(1), 92. https://doi.org/10.1186/s12951-017-0324-z

Baruah, I., Kashyap, C., Guha, A. K., & Borgohain, G. (2022). Insights into the interaction between polyphenols and β-lactoglobulin through molecular docking, MD simulation, and QM/MM approaches. *ACS Omega, 7*(27), 23083–23095. https://doi.org/10.1021/acsomega.2c00336

Chen, Y., Sun, Y., Ding, Y., Ding, Y., Liu, S., Zhou, X., Wu, H., Xiao, J., & Lu, B. (2024). Recent progress in fish oil-based emulsions by various food-grade stabilizers: Fabrication strategy, interfacial stability mechanism and potential application. *Critical Reviews in Food Science and Nutrition, 64*(6), 1677–1700. https://doi.org/10.1080/10408398.2022.2118658

Cilliers, F. P., Gouws, P. A., Koutchma, T., Engelbrecht, Y., Adriaanse, C., & Swart, P. (2014). A microbiological, biochemical and sensory characterisation of bovine milk treated by heat and ultraviolet (UV) light for manufacturing Cheddar cheese. *Innovative Food Science & Emerging Technologies, 23*, 94–106. https://doi.org/10.1016/j.ifset.2014.03.005

Ghelichi, S., Hajfathalian, M., Yesiltas, B., Sørensen, A. D. M., García-Moreno, P. J., & Jacobsen, C. (2023). Oxidation and oxidative stability in emulsions. *Comprehensive Reviews in Food Science and Food Safety, 22*(3), 1864–1901. https://doi.org/10.1111/1541-4337.13134

Gong, T., Tian, D., Hu, C. Y., Guo, Y. R., & Meng, Y. H. (2022). Improving antioxidant ability of functional emulsifiers by conjugating polyphenols to sodium caseinate. *LWT, 154*, Article 112668. https://doi.org/10.1016/j.lwt.2021.112668

Gulzar, S., Benjakul, S., & Hozzein, W. N. (2020). Impact of β-glucan on debittering, bioaccessibility and storage stability of skim milk fortified with shrimp oil nanoliposomes. *International Journal of Food Science & Technology, 55*(5), 2092–2103. https://doi.org/10.1111/ijfs.14452

Gunti, L., Dass, R. S., & Kalagatur, N. K. (2019). Phytofabrication of selenium nanoparticles from Emblica officinalis fruit extract and exploring its biopotential applications: Antioxidant, antimicrobial, and biocompatibility. *Frontiers in Microbiology, 10*, 931. https://doi.org/10.3389/fmicb.2019.00931

He, J., Wang, Z., Wei, L., Ye, Y., Din, Z. U., Zhou, J., … Cai, J. (2023). Electrospray-assisted fabrication of dextran-whey protein isolation microcapsules for the encapsulation of selenium-enriched peptide. *Foods, 12*(5), 1008. https://doi.org/10.3390/foods12051008

Jalalizand, F., & Goli, M. (2021). Optimization of microencapsulation of selenium with gum Arabian/Persian mixtures by solvent evaporation method using response surface methodology (RSM): Soybean oil fortification and oxidation indices. *Journal of Food Measurement and Characterization, 15*, 495–507. https://doi.org/10.1007/s11694-020-00659-y

Jia, X., Zhao, M., Xia, N., Teng, J., Jia, C., Wei, B., Huang, L., & Chen, D. (2019). Interaction between plant phenolics and rice protein improved oxidative stabilities of emulsion. *Journal of Cereal Science, 89*, Article 102818. https://doi.org/10.1016/j.jcs.2019.102818

Ju, M., Zhu, G., Huang, G., Shen, X., Zhang, Y., Jiang, L., & Sui, X. (2020). A novel Pickering emulsion produced using soy protein-anthocyanin complex nanoparticles. *Food Hydrocolloids, 99*, Article 105329. https://doi.org/10.1016/j.foodhyd.2019.105329

Keramat, M., Kheynoor, N., & Golmakani, M. T. (2022). Oxidative stability of Pickering emulsions. *Food Chemistry: X, 14*, Article 100279. https://doi.org/10.1016/j.fochx.2022.100279

Kheynoor, N., Jacquier, J. C., Khalesi, M., Mortazavian, A. M., & Golmakani, M. T. (2025). Formulation and characterization of sodium caseinate/phloretin complexes as antioxidant stabilizers in oil-in-water emulsions. *Foods, 14*(2), 236. https://doi.org/10.3390/foods14020236

Ks, S., Bimlesh, M., Rajan, S., & Rajesh, K. (2017). Preparation and functional characterization of whey protein-maltodextrin conjugates. *Res. Rev. J. Food Dairy Technol, 5*, 7–16.

Liu, K., Zha, X.-Q., Li, Q.-M., Pan, L.-H., & Luo, J.-P. (2021). Hydrophobic interaction and hydrogen bonding driving the self-assembling of quinoa protein and flavonoids. *Food Hydrocolloids, 118*, Article 106807. https://doi.org/10.1016/j.foodhyd.2021.106807

Low, L. K. (1992). Analysis of oils: Determination of peroxide value. In *laboratory manual on analytical methods and procedures for fish and fish products* (pp. C-7.1-C-7.4). Marine fisheries research department, southeast Asian fisheries development. Doi: hdl.handle.net/20.500.12066/6054.

Mariadoss, A. V. A., Saravanakumar, K., Sathiyaseelan, A., Naveen, K. V., & Wang, M. H. (2022). Enhancement of anti-bacterial potential of green synthesized selenium nanoparticles by starch encapsulation. *Microbial Pathogenesis, 167*, Article 105544. https://doi.org/10.1016/j.micpath.2022.105544

Mariadoss, A. V. A., Vinayagam, R., Senthilkumar, V., Paulpandi, M., Murugan, K., Xu, B. K. M. G., … David, E. (2019). Phloretin loaded chitosan nanoparticles augments the pH-dependent mitochondrial-mediated intrinsic apoptosis in human oral cancer cells. *International Journal of Biological Macromolecules, 130*, 997–1008. https://doi.org/10.1016/j.ijbiomac.2019.03.031

McClements, D. J. (2010). Emulsion design to improve the delivery of functional lipophilic components. *Annual Review of Food Science and Technology, 1*(1), 241–269. https://doi.org/10.1146/annurev.food.080708.100722

Meng, X., Liu, H., Dong, X., Wang, Q., Xia, Y., & Hu, X. (2022). A soft Pickering emulsifier made from chitosan and peptides endows stimuli-responsiveness, bioactivity and biocompatibility to emulsion. *Carbohydrate Polymers, 277*, Article 118768. https://doi.org/10.1016/j.carbpol.2021.118768

Nassar, A. A., Eid, A. M., Atta, H. M., El Naghy, W. S., & Fouda, A. (2023). Exploring the antimicrobial, antioxidant, anticancer, biocompatibility, and larvicidal activities of selenium nanoparticles fabricated by endophytic fungal strain Penicillium verhagenii. *Scientific Reports, 13*(1), 9054. https://doi.org/10.1038/s41598-023-35360-9

Salama, H. H., El-Sayed, H. S., Abd-Rabou, N. S., & Hassan, Z. M. (2021). Production and use of eco-friendly selenium nanoparticles in the fortification of yoghurt. *Journal of Food Processing and Preservation, 45*(6), Article e15510. https://doi.org/10.1111/jfpp.15510

Sepeidnameh, M., Hosseini, S. M. H., Niakosari, M., Mesbahi, G. R., Yousefi, G. H., Golmakani, M. T., & Nejadmansouri, M. (2018). Physicochemical properties of fish oil in water multilayer emulsions prepared by a mixture of whey protein isolate and water-soluble fraction of Farsi gum. *International Journal of Biological Macromolecules, 118*(Pt B), 1639–1647. https://doi.org/10.1016/j.ijbiomac.2018.07.007

Stani, C., Vaccari, L., Mitri, E., & Birarda, G. (2020). FTIR investigation of the secondary structure of type I collagen: New insight into the amide III band. *Spectrochimica Acta Part A: Molecular and Biomolecular Spectroscopy, 229*, Article 118006. https://doi.org/10.1016/j.saa.2019.118006

Su, Y. R., Tsai, Y. C., Hsu, C. H., Chao, A. C., Lin, C. W., Tsai, M. L., & Mi, F. L. (2015). Effect of grape seed Proanthocyanidin-gelatin colloidal complexes on stability and in vitro digestion of fish oil emulsions. *Journal of Agricultural and Food Chemistry, 63*(46), 10200–10208. https://doi.org/10.1021/acs.jafc.5b04814

Wang, R., Tian, Z., & Chen, L. (2011). A novel process for microencapsulation of fish oil with barley protein. *Food Research International, 44*(9), 2735–2741. https://doi.org/10.1016/j.foodres.2011.06.013

Yang, J., Ciftci, D., & Ciftci, O. N. (2024). Fortification of Milk with Omega-3 fatty acids using novel bioactive-carrier hollow solid lipid Micro-and nanoparticles for improved Omega-3 stability and bioaccessibility. *ACS Food Science & Technology, 4*(4), 813–820. https://doi.org/10.1021/acsfoodscitech.3c00141

Zhang, X., Wang, C., Qi, Z., Zhao, R., Wang, C., & Zhang, T. (2022). Pea protein based nanocarriers for lipophilic polyphenols: Spectroscopic analysis, characterization, chemical stability, antioxidant and molecular docking. *Food Research International, 160*, Article 111713. https://doi.org/10.1016/j.foodres.2022.111713

Zhu, Y., Sun, X., Luo, X., Ding, J., Fan, F., Li, P., Shen, X., & Fang, Y. (2022). Encapsulation of selenium-containing peptides in xanthan gum-lysozyme nanoparticles as a powerful gastrointestinal delivery system. *Food Research International, 156*, Article 111351. https://doi.org/10.1016/j.foodres.2022.111351